Quaternary Science Reviews 29 (2010) 2473–2483

Contents lists available at ScienceDirect

Quaternary Science Reviews

journal homepage: www.elsevier.com/locate/quascirev

Eastern Mediterranean surface water Nd during Eemian sapropel S5: monitoring northerly (mid-latitude) versus southerly (sub-tropical) freshwater contributions

A.H. Osborne [a], G. Marino [b], D. Vance [a,*], E.J. Rohling [c]

[a] Bristol Isotope Group, Department of Earth Sciences, University of Bristol, Bristol BS8 1RJ, United Kingdom
[b] Institut de Ciència i Tecnologia Ambientals (ICTA), Universitat Autònoma de Barcelona, Bellaterra, Spain
[c] School of Ocean and Earth Science, National Oceanography Centre, Southampton SO14 3ZH, United Kingdom

ARTICLE INFO

Article history:
Received 14 December 2009
Received in revised form
12 May 2010
Accepted 13 May 2010

ABSTRACT

A well developed sapropel (S5) was deposited in the eastern Mediterranean during the Last Interglacial (Eemian), 124–119 ka. Freshwater contributions to the basin at this time can be traced using the isotopic composition of Nd in planktonic foraminifera. This enables differentiation between radiogenic sources to the south, under the influence of the African monsoon, and unradiogenic sources to the north, relating to the mid-latitude westerlies. Here we compare new Nd data, from a core in the southeast Aegean Sea, with published data from the Ionian and Levantine Seas. Shifts towards more radiogenic Nd in the lower and middle parts of sapropel S5 are most pronounced in the Ionian Sea record, with ε_{Nd} and $\delta^{18}O_{G.\ ruber}$ co-varying more closely here than in the Levantine and Aegean Seas. This is consistent with a freshwater source proximal to the Ionian Sea site, likely indicating a substantial reactivation of rivers flowing northward from the central Saharan watershed. The lack, during S5 deposition, of a noticeable shift towards more unradiogenic Nd in the Aegean record would exclude a large influx of water from the northern borders of the eastern Mediterranean during sapropel deposition. These findings support a scenario whereby the Last Interglacial eastern Mediterranean was influenced strongly by the remote effects of an intensified African monsoon, with more local precipitation in the northern borders contributing relatively little to the sea surface composition.

1. Introduction

The flux of material from the continents to the oceans via fluvial and aeolian transport is driven to some extent by climate (e.g. Falkowski et al., 1998; Riebe et al., 2004; Vance et al., 2009). The isotopic composition of trace elements in ocean sediments can be used to monitor these climate-driven changes in continental weathering (Frank, 2002; Reynolds et al., 2004). Elements like Sr, with long residence times in the oceans, are used as long-term indicators of global weathering rates (Frank, 2002). Others, such as Nd, Hf and Pb have oceanic residence times which are comparable to, or shorter than, both the duration of ocean mixing and the timescale on which Quaternary climate change operates. They in contrast to Sr can, therefore, be used to monitor regional weathering inputs as well as ocean circulation (Frank, 2002; Reynolds et al., 2004; Piotrowski et al., 2005; Foster and Vance, 2006).

The Mediterranean Sea, at the boundary between the sub-tropical and mid-latitudes zones (Lionello et al., 2006), is ideally situated to record in its sediments changes in climatic and other environmental factors on continents dominated by these two major climate regimes. High-resolution paleoceanographic records are available through the high sediment accumulation rates in the Mediterranean (e.g. Sprovieri et al., 2003, 2006; Martrat et al., 2004; Marino et al., 2007). Finally, the basin features a circulation regime that is highly sensitive to changes imposed by the boundary conditions on the surrounding continents, notably the supply of freshwater (Rohling et al., 2006; Marino et al., 2007; Skliris et al., 2007). Although changes in the freshwater balance through time can be reconstructed from hydrological tracers like oxygen isotopes (e.g. Rohling, 1999; Rohling and De Rijk, 1999), such approaches carry little provenance information. Such information is essential in the Mediterranean, where changes in freshwater supply can be driven by very different climatic processes, namely changes in the activity of the westerly regime over the European continent versus variations in sub-tropical and tropical climate over the African landmass (Tzedakis, 2007).

The distribution of crustal residence ages in the bordering landmasses is such that inputs from different regions are distinguishable on the basis of their Nd isotopic composition (Fig. 1; Scrivner et al., 2004; Tachikawa et al., 2004; Jeandel et al., 2007).

* Corresponding author. Tel.: +44 117 954 5418; fax: +44 117 925 3385.
E-mail address: d.vance@bristol.ac.uk (D. Vance).

0277-3791/$ – see front matter © 2010 Elsevier Ltd. All rights reserved.
doi:10.1016/j.quascirev.2010.05.015

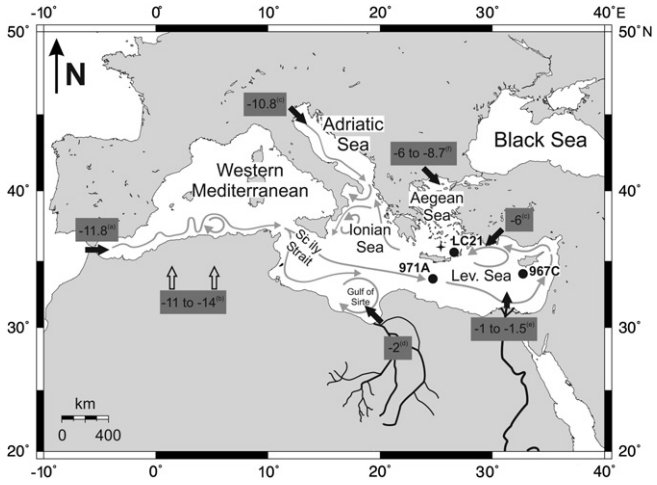

Fig. 1. Map of the Mediterranean Sea and surrounding continents, showing locations of major features and the three core sites (black dots) discussed in the text. Also shown is a reconstruction of the fossil river channel network in the central eastern Sahara (Rohling et al., 2002 adapted from Pachur and Altmann, 2006), and the main Nile channel. The grey arrows show the major patterns of surface water circulation in the Mediterranean Sea (redrawn from Pinardi and Masetti, 2000). Values in the dark grey boxes indicate ε_{Nd} of inputs to the Mediterranean. The westernmost solid arrow represents Atlantic surface waters entering the Mediterranean via the Strait of Gibraltar, (a) Spivack and Wasserburg (1988). The open arrows denote aeolian dust deposited across the surface of the Mediterranean, (b) Grousset et al. (1992), Henry et al. (1994). Fluvial inputs to the eastern Mediterranean, past and present, are indicated by solid arrows, Po and Turkish rivers (c) Frost et al. (1986); ancient Libyan rivers (d) Osborne et al. (2008); Nile (e) Scrivner et al. (2004); Northern borderland rivers via the Aegean (f) Freydier et al. (2001), Weldeab et al. (2002a). The star indicates the nearest available surface water ε_{Nd} for the LC21 site (Tachikawa et al., 2004).

Moreover, the semi-enclosed nature of the Mediterranean Sea allows for a close monitoring of the Nd budget (Frost et al., 1986), although there is some uncertainty surrounding the importance of contributions from partially dissolved riverine particulates (Tachikawa et al., 2004).

In this paper we present a new record of neodymium isotopes in planktonic foraminifera from the Last Interglacial (Eemian) sapropel S5 sediments in a core in the southeastern Aegean Sea. We compare these results with published data for dissolved Nd in the present-day Mediterranean (Tachikawa et al., 2004), and with other Last Interglacial Nd isotope records from sediment cores in the eastern Levantine and the western Ionian Seas (Scrivner et al., 2004; Osborne et al., 2008). The geographical distribution of the cores allows for monitoring of freshwater inputs from monsoonal (tropical) versus mid-latitude sources.

2. Regional setting

Fig. 1 illustrates the position of the three cores discussed in this study and shows the basin scale cyclonic pattern of surface water circulation in the Mediterranean, which responds to the large-scale atmospheric processes. Briefly, surface water derived from the Atlantic Ocean circulates eastward along the southern sector of the Mediterranean in the form of jet-like currents (Pinardi and Masetti, 2000), encountering first the region of ODP 971A, before turning northwards across 967C and then returning westwards across LC21, under the influence of gyres in the eastern Mediterranean (Roussenov et al., 1995; Pinardi and Masetti, 2000).

Previous studies have emphasized the sensitivity to climate forcing of deep water formation in the Mediterranean Sea, and notably in the Aegean Sea (e.g. Marino et al., 2007; CIESM, 2009). This is best exemplified by the severe perturbation that occurred in the late 1980s to early 1990s, the Eastern Mediterranean Transient (EMT) (Roether et al., 2007). During the EMT, following a salt build up in the Ionian and Levantine Seas (Malanotte-Rizzoli et al., 1999; Skliris et al., 2007), large volumes of unusually dense and saline waters spilt out of the Aegean Sea. The latter, for approximately a decade, became the main source of eastern Mediterranean deepwaters, replacing the previously dominant Adriatic Sea bottom waters (Roether et al., 1996, 2007). Changes in the opposite sense, through the development of a relatively fresh upper layer, have led to a reduction in deep water formation across the entire eastern Mediterranean and, via the resultant starvation of oxygen in the bottom water, to the deposition of discrete layers that are enriched in organic matter ('sapropels') (e.g. Marino et al., 2007).

A number of possible scenarios for the increased freshwater supply to the eastern Mediterranean have been put forward to explain bottom water stagnation during sapropel formation (see Cramp and O'Sullivan, 1999 for a review). The possible impacts of the Black Sea overflow (Olausson, 1961) and continental ice-caps melting to the north of the Mediterranean (Ryan, 1972) have been discounted due to inconsistencies between the proposed driver and the geographic and temporal distribution of sapropels (Rossignol-Strick et al., 1982; Hilgen et al., 1997; Sperling et al., 2003). The hypotheses that remain in contention broadly divide into two: those controlled by high- to mid-latitude climatic drivers and that involve enhanced freshwater supply from the northern borderlands or directly over the Mediterranean itself (e.g. Kotthoff et al., 2008), versus those that involve tropical drivers and increased freshwater supply from either the Nile or from broader regions along the North African margin (e.g. Rohling et al., 2002). With regard to our purposes here, these two drivers should in principle have different and identifiable impacts on the Mediterranean Nd isotopic budget and they will be discussed in more detail below.

Increases in precipitation in the Northern Borderlands of the Eastern Mediterranean (NBEM) concurrent with sapropel deposition have been proposed on the basis of a number of approaches (e.g. Cramp et al., 1988; Zanchetta et al., 2007; Kotthoff et al., 2008). Based on available palaeoclimatological data, Rohling and Hilgen (1991) interpreted potential precipitation increases in the NBEM as a result of secondary depression tracks in the region in the wake of a northward movement of the main Atlantic depression track (Kutzbach and Guetter, 1986). Summer precipitation could have been further strengthened by additional evaporation from warm waters as a result of an insolation-induced increase in temperature contrast across the Gulf Stream and North Atlantic Drift (Rohling, 1994).

In contrast, the strong temporal correlation between sapropel occurrence and precession minima-related insolation maxima in the Northern Hemisphere (Rossignol-Strick et al., 1982; Rossignol-Strick, 1983, 1985) has led to the suggestion that the freshwater balance of the (eastern) Mediterranean, and thus sapropel formation, is fundamentally controlled by changes in supply of monsoon-fuelled freshwater from the North African continent. This hypothesis has found two expressions – changes in freshwater supply from the Nile point source (Rossignol-Strick et al., 1982; Rossignol-Strick, 1983; Freydier et al., 2001; Scrivner et al., 2004) versus increased supply from the wider North African margin through, for example, radar-imaged fossil river channels extending across the Libyan Sahara (Rohling et al., 2002, 2004; Larrasoaña et al., 2003; Osborne et al., 2008).

A concentration of the biggest surface ocean $\delta^{18}O$ shifts in the region south of Crete and the presence of large palaeo-river channels crossing Libya point to a substantial influx of freshwater from the wider North African margin during sapropel deposition (Rohling et al., 2002). A source of freshwater and river sediment local to the eastern Ionian Sea has also been suggested by Fontugne

et al. (1994), Krom et al. (1999b), Freydier et al. (2001) and Scrivner et al. (2004).

These ideas find support in the apparent reduction in the contribution of Saharan dust to the Mediterranean during sapropel deposition (Krom et al., 1999a,b; Weldeab et al., 2002b), since such changes are presumably driven by wet-dry cycles in the Sahara and the corresponding changes in vegetative cover. Since the majority of dust arriving in the Mediterranean is delivered from the area north of 21°N (Larrasoaña et al., 2003), a decrease in production indicates that wetter conditions had extended northwards of the present-day limit of the Sahel at 18°N, crossing the central Saharan watershed at around 21°N. Orbitally forced models of mid-Holocene climate simulate an increase in the amount and northerly extent of African monsoon rains (e.g. Kutzbach and Liu, 1997). However, even models which include ocean and vegetation feedbacks are not able to fully reproduce conditions that agree with pollen data, i.e., they do not support an extension of the Sahel to 23°N (Jolly et al., 1998; Claussen et al., 1999). Other evidence for greater precipitation in the region comes from lake level records (Yu and Harrison, 1996), the fossilised remains of crocodiles and fish (Pachur and Altmann, 2006) and the groundwater ages (Sonntag et al., 1978; Sultan et al., 1997).

3. Neodymium in the Mediterranean

While the regional pattern of foraminiferal $\delta^{18}O$ is a strong indicator of freshwater input, this alone is insufficient to pinpoint the source of that freshwater, as foraminiferal $\delta^{18}O$ is not a conservative property in the surface ocean and is affected by changes in the balance of evaporation, precipitation and runoff, and the $\delta^{18}O$ of each of these terms (Rohling and Bigg, 1998). The isotopic composition of neodymium can be used as an alternative tool that links source area and ocean basin and has, moreover, the advantage over other proxies of being able to distinguish between catchments of differing rock type (Goldstein and Hemming, 2003). The distribution of crustal ages around the eastern Mediterranean makes it possible to use their Nd isotopic composition to distinguish between regional inputs (Fig. 1; Scrivner et al., 2004; Tachikawa et al., 2004; Jeandel et al., 2007). A greater contribution of radiogenic inputs from the south would imply an increase in the strength and northward extent of the African monsoon, whereas an enhanced supply of unradiogenic inputs from the northern borders would imply an increase in precipitation from mid-latitude weather systems. Increased precipitation directly over the Mediterranean basin should have little effect on the Nd composition of surface waters.

4. Neodymium in planktonic foraminifera

Reductive–oxidatively (RO) cleaned planktonic foraminifera from core tops have been shown to record the ε_{Nd} (parts per 10,000 deviation of the measured $^{143}Nd/^{144}Nd$ ratio from the chondritic uniform reservoir) of surface waters (Vance and Burton, 1999; Burton and Vance, 2000; Vance et al., 2004). High concentrations of rare earth elements (REEs) are associated with Fe–Mn oxide phases (Bau et al., 1996) which form on the surface of foraminifera during diagenesis (e.g. Palmer, 1985; Haley and Klinkhammer, 2002; Vance et al., 2004; Haley et al., 2005) and have presented significant problems for the analysis of some other trace elements in foraminifera, such as Cd (Boyle, 1983). However, several observations negate the importance of these coatings for the Nd inventory of sedimentary foraminifera. First, post-depositional addition of Nd from bottom and/or pore waters is inconsistent with core top planktonic foraminifera recording surface water ε_{Nd} values (Vance and Burton, 1999; Burton and Vance, 2000; Vance et al., 2004). Most importantly, however, the Nd/Mn ratios obtained for uncleaned sedimentary foramininfera, are up to two orders of magnitude greater than for other Fe–Mn oxides (Vance et al., 2004), ruling out the possibility of any significant contamination from such coatings and negating the impact of preferential re-adsorption of REEs during cleaning.

Instead, Vance et al. (2004) and Haley et al. (2005) speculated that the high REE concentration in foraminifera was a result of the affinity of REEs to organic matter, which includes the proteins used by foraminifera to acquire calcium ions to build their shells (Evans, 2003) and which is preserved as intra-test lamellae (e.g. Lipps, 1973). Spatially-resolved analyses of foraminiferal shells have confirmed that there are differences in the concentrations of trace elements in different layers of foraminiferal calcite (e.g. Erez, 2003 and references therein). Recent work by Martínez-Botí et al. (2009) on multiple species of plankton tow and core-top planktonic foraminifera supports the presence of an isotopically homogeneous Nd 'pool' associated with intra-test organic material, acquired in surface waters during foraminferal growth and then protected from aggressive cleaning processes and diagenetic effects by the surrounding calcite structure, in a similar way to that which has been recently proposed for nitrogen (Ren et al., 2009). Hence, ε_{Nd} in planktonic foraminifera can be used in down-core studies to investigate palaeo-surface waters, and indeed ε_{Nd} changes in planktonic foraminifera have been shown to be coherent with other indicators for palaeoclimatic change (Vance and Burton, 1999; Burton and Vance, 2000; Scrivner et al., 2004).

5. Materials and methods

Here we compare Nd in planktonic foraminifera from Last Interglacial sapropel S5 in the eastern Levantine Sea (ODP 967C, Scrivner et al., 2004) and in the western Ionian Sea (ODP 971A, Osborne et al., 2008) with new data from S5 in core LC21 from the southeastern Aegean (35° 40′N, 26° 35′E, 1522 m water depth). Whereas the position of ODP cores 967C and 971A makes them suitable for investigating runoff from African catchments, the location of LC21 in the southeastern Aegean is such that it should be able to capture more of a signal from the NBEM.

Mixed samples of *Globigerinoides ruber* (white) and *Orbulina universa* were hand-picked from the 125–355 μm size fraction from key intervals in sediments before, during and after the interglacial sapropel S5, selected using a previously published $\delta^{18}O_{G.\ ruber}$ record (Marino et al., 2007). *G. ruber* dwells in the upper 50 m of the

Table 1
Nd and Sm isotopic data for LC21 foraminifera.

LC21 depth (cm)	Species[a]	ε_{Nd}[b]	2σ	[Nd] ppm	$^{147}Sm/^{144}Nd$
835–850.5	Mixed	−5.05	0.33	0.62	0.1384
837–839	Mixed	−4.91	0.21	1.26	0.1423
855.5–869.5	Mixed	−6.05	0.30	1.50	0.1405
865.5–880.5	Mixed	−4.25	0.32	1.31	0.1453
876–880	Mixed	−3.49	0.38	0.68	0.1663
890–940	Mixed	−5.82	0.27	0.15	0.1406
895	Mixed	−2.53	0.91		0.1667
945–960	Mixed	−4.88	0.31	0.24	0.1224
960	Mixed	−3.70	0.73	0.75	0.1453
965–985	Mixed	−5.65	0.49	0.21	0.1457
1000–1044	Mixed	−4.08	0.79	0.35	0.1430
1008.25–1044	Mixed	−4.75	0.25	0.47	0.1418

[a] "Mixed" species refers to samples containing both *G. ruber* (white) and *O. universa*.
[b] $^{143}Nd/^{144}Nd$ is reported in ε units (ε_{Nd}) relative to the chondritic uniform reservoir (CHUR). $\varepsilon_{Nd} = [(^{143}Nd/^{144}Nd_{measured})/(^{143}Nd/^{144}Nd_{CHUR}) - 1] \times 10{,}000$. The reported 2σ uncertainty is the internal error. With reproducibility of standards is at the <0.2 ε unit level, the internal error for these small samples dominates the uncertainty.

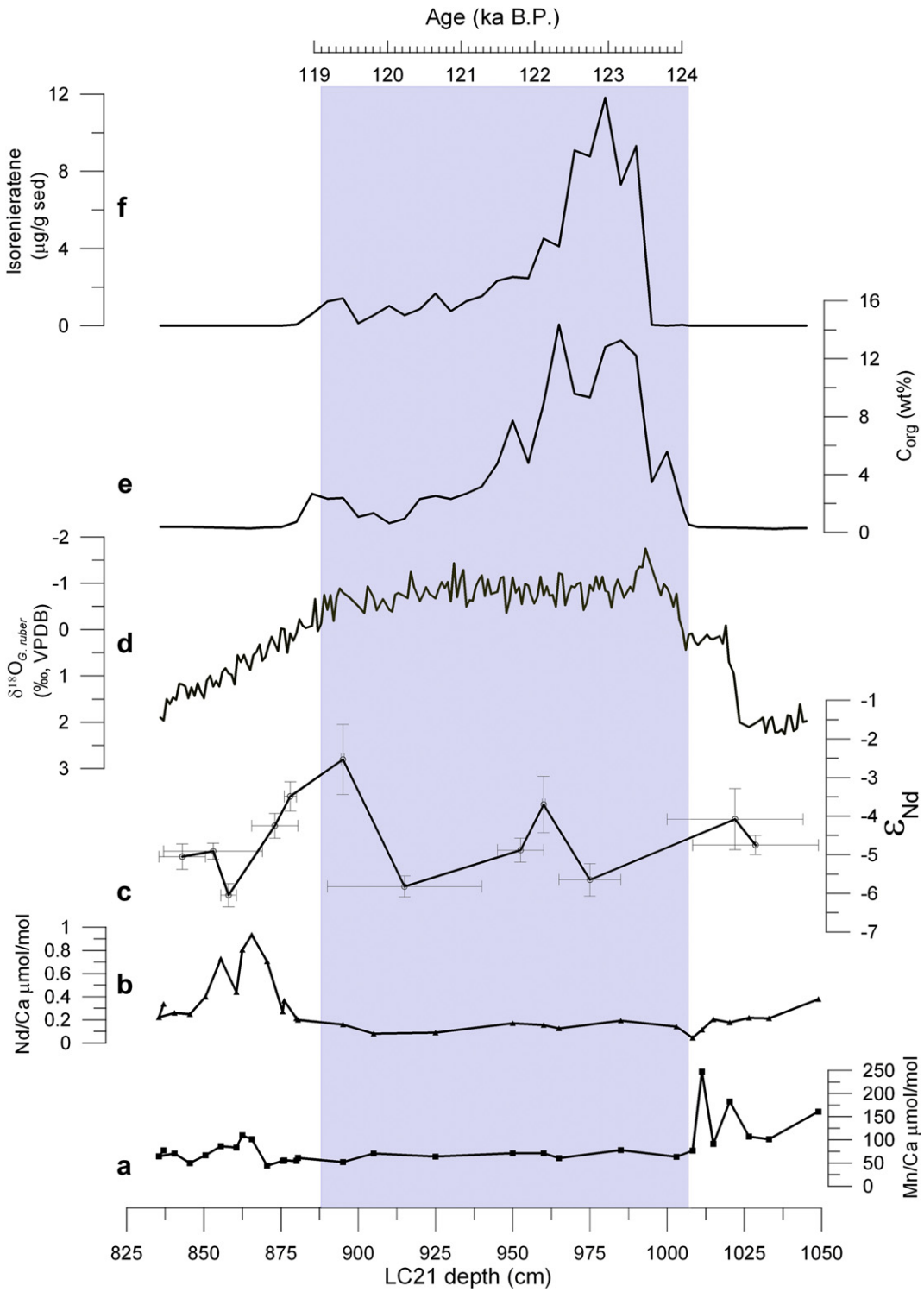

Fig. 2. New and previously published geochemical proxies across sapropel S5 in core LC21. a), b): Mn/Ca and Nd/Ca for mixed samples of *Globigerinoides ruber* and *Orbulina universa*. Uncertainty on these measurements is between 2% and 5% and therefore comparable with symbol size. c): ε_{Nd} record for mixed samples of *G. ruber* and *O. universa*, vertical error bars are 2σ error, horizontal error bars indicate the depths across which samples were combined in order to obtain sufficient Nd for analysis. d) $\delta^{18}O$ record for *G. ruber* (Marino et al., 2007). e) Total organic carbon content (C_{org}) (Marino et al., 2007). f) Isorenieratene abundances (Marino et al., 2007). The grey shaded area indicates the visual extent of S5 in LC21. The age scale is based on ages for the onset and end of S5, as inferred from the comparison of the $\delta^{18}O$ record with that of U–Th-dated Soreq Cave speleothems (Bar-Matthews et al., 2000). VPDB-Vienna Peedee belemnite.

water column and has a peak abundance in the Mediterranean in late summer (Pujol and Vergnaud-Grazzini, 1995). *O. universa* is similarly a summer species, with highest occurrence between 50 and 100 m water depth in the eastern Mediterranean (Pujol and Vergnaud-Grazzini, 1995). Rohling et al. (2004) established that these broad habitat characteristics applied also at the time of the deposition of S5. Use of a mixed sample of the two species was based on the findings of Scrivner et al. (2004), who showed that there was no difference in the ε_{Nd} between the two species in samples taken from ODP core 967C.

All picked foraminiferal samples underwent reductive-oxidative cleaning (Boyle and Keigwin, 1985; Vance et al., 2004). Trace element concentrations were measured on a ThermoFinnigan Element2 Inductively Coupled Plasma Mass Spectrometer (ICPMS) and the Nd and Sm isotope compositions were measured on a ThermoFinnigan Neptune Multi Collector ICPMS, both at the University of Bristol. For the majority of depth intervals in LC21, scarcity of foraminifera and/or low concentration of Nd in the foraminiferal calcite made it necessary to combine (several) adjacent samples in order to successfully analyse ε_{Nd}. Procedural blanks were between 10–20 pg Nd and all measurements were corrected assuming a blank of average crustal $\varepsilon_{Nd} = -10$. The smallest sample contained 500 pg Nd which resulted in a blank correction of +0.3 ε units. Multiples of eight samples were bracketed with a La Jolla standard of known $^{143}Nd/^{144}Nd$ ratio (0.511856) and additional standard measurements were taken at the beginning and end of each analytical session. External reproducibility of repeated measurements of a 50 ppb La Jolla Nd standard (0.3 ml used per analysis, equivalent to 17 ng total Nd measured) within one session was between 8 and 16 ppm (2σ). For the much smaller samples analysed here, the internal uncertainty becomes the greater source of error and reproducibility less important. However, for two sessions, 10 ppb standards were analysed ($n = 10$ for both, again 0.3 ml of solution analysed, equivalent to 3 ng Nd) and gave 0.511856 ± 23 and 0.511868 ± 27. The reproducibility of these small standards is close to the internal uncertainties reported here for samples that are comparable in size. Primary corrections for ICPMS mass bias used $^{146}Nd/^{144}Nd = 0.7219$ and secondary corrections used $^{142}Nd/^{144}Nd = 1.141876$ (Vance and Thirlwall, 2002). The precision of Nd and Sm concentrations was approximately 5%. $^{147}Sm/^{144}Nd$ measurements were precise to 0.5% (Vance et al., 2004) (Table 1).

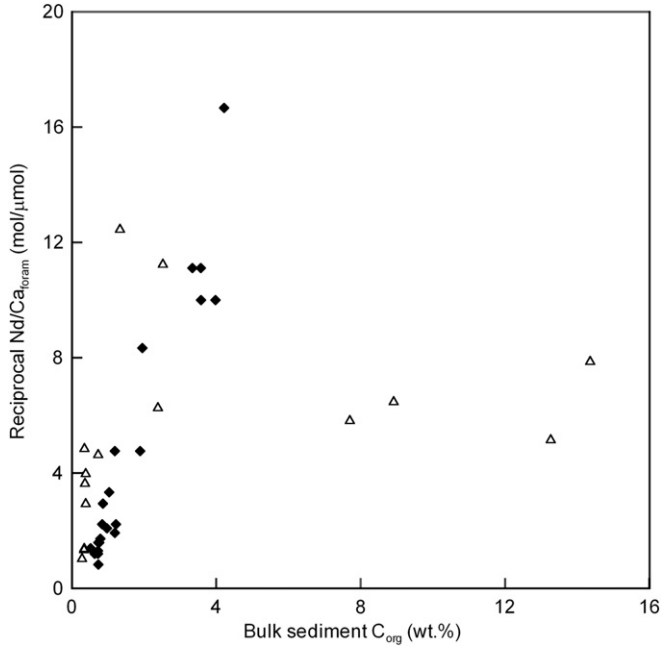

Fig. 3. Total organic carbon (C_{org}) in bulk sediment plotted against reciprocal Nd/Ca ratio in foraminiferal calcite of mixed *G. ruber* and *O. universa* samples from the same horizons. Open triangles are from sapropel S5 in core LC21, Aegean Sea (C_{org} from Marino et al., 2007, Nd/Ca from this study). Filled diamonds are from sapropel layer S1 in ODP core 967D, Levantine Basin (Vance et al., 2004), with the omission of one horizon containing very low Nd/Ca.

6. Results and discussion

6.1. Variability in Nd/Ca in LC21 foraminifera

The Nd contents of the foraminifera measured from LC21 vary by a factor of nearly 20, from 0.05–0.93, but there is some pattern to this variation. Specifically, Nd/Ca ratios tend to be higher outside the sapropel and are at their lowest within (Fig. 2). Vance et al. (2004) presented Nd/Ca ratios for foraminiferal calcite extracted from S1 in ODP 967D. These latter samples had an almost identical range in Nd/Ca (0.06–1.21) to that observed here for S5 in LC21. Furthermore, the data for S1 in 967D show exactly the same pattern as seen here, with high values outside the sapropel and lowest values within. Indeed, Vance et al. (2004) noted a tight inverse correlation between the total organic carbon (C_{org}) content of bulk sediments in 967D S1 and the Nd/Ca ratio of foraminiferal calcite. C_{org} contents of S5 bulk sediments in LC21 extend up to nearly 15%, whereas those for S1 at 967C are never higher than 4%. Fig. 3 demonstrates, however, that the data for foraminiferal Nd/Ca in S5 from LC21 exhibit the same covariance with C_{org} for those samples with less than 4% C_{org}. This relationship breaks down for

Table 2
Mn/Ca and Nd/Ca data for foraminifera in core LC21.

LC21 depth (cm)	Species[a]	Mn/Ca[b] (μmol/mol)	Nd/Ca[b] (μmol/mol)
835.5	Mixed	64.60	0.22
837	Mixed	77.51	0.34
840.5	Mixed	70.87	0.26
845.5	Mixed	50.01	0.25
850.5	Mixed	66.80	0.40
855.5	Mixed	86.53	0.73
860.5	Mixed	83.34	0.44
862.5	Mixed	109.85	0.81
865.5	Mixed	101.35	0.93
870.5	Mixed	44.18	0.70
875.5	Mixed	54.94	0.27
876	Mixed	55.22	0.37
880	Mixed	54.63	0.21
880.5	Mixed	60.71	0.20
885	Mixed	61.13	
895	Mixed	52.30	0.16
900	Mixed	31.28	
905	Mixed	64.75	
905	Mixed	70.53	0.08
925	Mixed	64.00	0.09
930	Mixed	34.45	
945	Mixed	67.44	
950	Mixed	54.20	
950	Mixed	71.11	0.17
955	Mixed	70.76	
960	Mixed	60.94	
960	Mixed	71.17	0.15
965	Mixed	49.76	
965	Mixed	60.38	0.13
980	Mixed	77.07	
985	Mixed	77.89	0.19
990	Mixed	83.72	
1000	Mixed	38.12	
1003	Mixed	63.27	0.14
1008.25	Mixed	76.47	0.05
1011.25	Mixed	247.08	0.11
1015.00	Mixed	91.25	0.20
1020.25	Mixed	182.94	0.18
1026.5	Mixed	107.36	0.22
1033.00	Mixed	101.32	0.21
1049.00	Mixed	161.02	0.38

[a] "Mixed" species refers to samples containing both *G. ruber* (white) and *O. universa*.
[b] Mn/Ca and Nd/Ca measured by ICP-MS. An initial analysis determined rough Ca concentrations while subsequent dilution and re-analysis matched Ca concentrations in samples and standards. Consistency standards were measured in each analytical session and yield a long-term reproducibility of 2–5% for Mn/Ca (depending on measured Mn/Ca) and 3–5% for Nd/Ca.

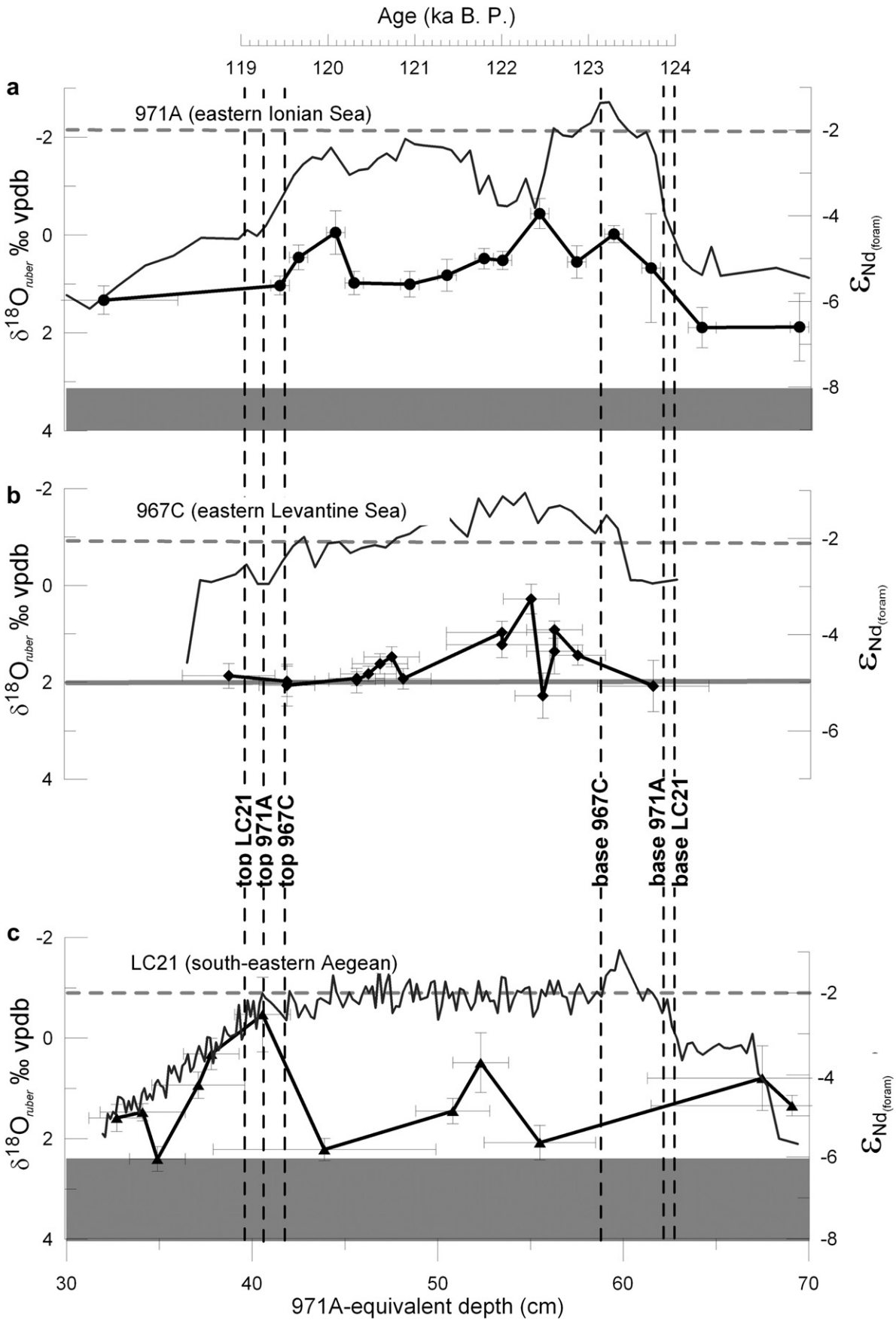
Age (ka B. P.)
119
120
121
122
123
124
a
971A (eastern Ionian Sea)
b
967C (eastern Levantine Sea)
c
LC21 (south-eastern Aegean)
δ18Oruber ‰ vpdb
εNd(foram)
top LC21
top 971A
top 967C
base 967C
base 971A
base LC21
971A-equivalent depth (cm)

samples with a greater proportion of C_{org}, where Nd/Ca are relatively constant around 0.1–0.2 (Table 2).

All the samples analysed here and in Vance et al. (2004) have been cleaned with an oxidative approach, so that any organic matter that the foraminifera contain, and any Nd associated with it, is removed before dissolution of foraminiferal calcite and analysis of Nd/Ca ratios. Vance et al. (2004) speculated that Nd is associated with organic matter in sapropel foraminifera and, because of the reducing conditions in deepwater and in the sediments in which the foraminifera are contained, remains in this form so that it is removed by this cleaning, leading to low Nd/Ca ratios. In this view, Nd associated with organic matter in foraminifera that are buried beneath an oxic water column is removed during oxidation of the organic matter, and transfer of this Nd to a phase in the foraminiferal test might lead to high Nd/Ca in all foraminiferal samples in oxic sediments.

Of course, all the above remains speculation, but the data for LC21 are broadly consistent with the above hypothesis, and it is an idea that can be tested by future work. It is also broadly consistent with the suggestion of Haley et al. (2005) and Martínez-Botí et al. (2009) that Nd in foraminiferal calcite may originally be acquired in the surface ocean through binding to organic matter.

6.2. The Aegean Nd isotope record

New Nd isotope data for sapropel S5 from core LC21 in the southeast Aegean complement previously published Nd isotope data from ODP cores 971A and 967C in the Ionian and Levantine Seas, respectively (Scrivner et al., 2004; Osborne et al., 2008). Although the resolution of data from LC21 is limited by the low concentration of Nd in the foraminiferal calcite, these records can be used in conjunction with the very high-resolution $\delta^{18}O_{G.\ ruber}$ data from this core (Marino et al., 2007) in order to investigate the impact of local (NBEM) versus distal (North African margin) freshwater sources. From the results obtained we note that during S5 in LC21 (Fig. 2) there is no noticeable shift towards more unradiogenic Nd in the sapropel layer. Below the sapropel, ε_{Nd} is -4.5 ± 0.8, which is at least 1 ε unit less negative than the closest available measurements of modern surface water ε_{Nd} (-6.2 ± 0.4 to -7.9 ± 0.2; Tachikawa et al., 2004) ~130 km northwest of LC21. This may be because surface water ε_{Nd} had already begun to change from the 'ambient' (i.e. non-sapropel) composition. Alternatively, the surface water in this location, which is thought to have been supplied by northward flowing Levantine surface water during S5 (Marino et al., 2007) as it is today (Theocharis et al., 2002), may have had an ε_{Nd} closer to -5 as measured in the eastern Mediterranean (Scrivner et al., 2004). ε_{Nd} values are between -3.7 ± 0.7 and -5.8 ± 0.3 throughout the lower and middle parts of the LC21 S5. Ten centimeters below the top of S5, the foraminiferal ε_{Nd} value shows an excursion that peaks at -2.5 ± 0.9. This is the least negative ε_{Nd} value yet observed in any of the Last Interglacial records for LC21, 971A or 967C (Scrivner et al., 2004; Osborne et al., 2008). ε_{Nd} values drop sharply in the overlying sediments, to a profile minimum of -6.1 ± 0.3 approximately 30 cm above the sapropel. There is a small rebound above this in the uppermost measurements, which, at -5.1 ± 0.3, are comparable to the values immediately below the sapropel.

Due to the basin wide counterclockwise circulation, the region around LC21 receives Levantine Surface and Intermediate water, both of which form in the nearby Rhodes Gyre (Theocharis et al., 2002). The closest measurement of ambient sea surface ε_{Nd} composition is ~130 km to the northwest of LC21 (Tachikawa et al., 2004) and may come under the influence of eastward spreading Modified Atlantic Water during the summer, as observed during September 1994 by the PELAGOS III cruise (Theocharis et al., 1999). An examination of salinity and temperature data from the closest available World Ocean Database sites (Boyer et al., 2006) was not sufficient to distinguish whether or not LC21 and the nearest sea surface ε_{Nd} measurement (Tachikawa et al., 2004) were affected by the same surface water mass. Assuming a background ε_{Nd} of -6 to -8, this region experienced a movement towards more radiogenic ε_{Nd} values prior to the sapropel and twice within the sapropel, returning to background levels twice. Even if the ambient surface waters were actually closer to the eastern Mediterranean ε_{Nd} value of -5 (Scrivner et al., 2004), then there is still very little in the LC21 record to suggest any significant shift towards more unradiogenic Nd that might be caused by an increased input from the NBEM.

6.3. Comparison between Mediterranean ε_{Nd} records

Direct comparison of palaeoproxy records for sapropel S5 from 971A, LC21 and 967C is possible as the latter two cores have previously been correlated with the "master stratigraphy" of 971A (Cane et al., 2002; Rohling et al., 2002; Marino et al., 2007) (Fig. 4). The ε_{Nd} records for 971A and 967C were recently used to make observations about the relative influence of freshwater inputs from the Nile and from the wider North African margin during S5 (Osborne et al., 2008). There was a much greater change in ε_{Nd} for 971A than for 967C. In absolute terms, there is a shift of 4–5 ε units in 971A during S5, much greater than the change of 1.7 ε units in 967C (Osborne et al., 2008). This work supported the Rohling et al. (2002) hypothesis that an orbitally forced increase in the northerly extent of the African monsoon during the Last Interglacial maximum brought the rain belt across the Central Saharan watershed and fed radar-imaged fossil river channels which extended all the way to the Gulf of Sirte on the Mediterranean coast (McCauley et al., 1982, 1995) (Fig. 1).

Scrivner et al. (2004) commented that the seemingly slow response of ε_{Nd} in 967C compared to the rapid change in $\delta^{18}O_{G.\ ruber}$ at the start of S5 deposition indicated that there may have been a non-radiogenic source of freshwater to the basin at this time. The White Nile contributes approximately 30% of the annual Nile River discharge and 3.5% of the total sediment, and discharge is fairly consistent throughout the year (Adamson et al., 1980). The Nd composition of the White Nile dissolved load is very unradiogenic, at ε_{Nd} around -16 (Scrivner, 2005). In contrast, the Blue Nile contribution is highly seasonal and very radiogenic (ε_{Nd} ~0 to +2, Scrivner, 2005), supplying nearly 70% of the water discharged during the season of strongest African monsoon rainfalls (summer), and 72% of the total annual sediment (Adamson et al., 1980). The Atbara is similarly radiogenic (ε_{Nd} ~ +1.6, Scrivner, 2005)

Fig. 4. $\delta^{18}O$ and ε_{Nd} data for foraminifera across sapropel S5 from three eastern Mediterranean cores, using the common depth scale of Cane et al. (2002), Rohling et al. (2002) and Marino et al. (2007). The horizontal dashed grey lines represent ε_{Nd} of Nile and putative North African rivers (Scrivner et al., 2004; Osborne et al., 2008). The horizontal grey bars indicate the closest available present-day sea surface ε_{Nd} for each site (Tachikawa et al., 2004), although, dependent on which water mass is above LC21, sea surface ε_{Nd} at this location could be closer to -5. The vertical dashed black lines represent the base and top of the visible extent of dark sapropel sediments in LC21, 971A and 967C as labeled (Rohling et al., 2002; Marino et al., 2007) and the timescale is based on a sapropel age of 124–119 ka (Bar-Matthews et al., 2000). a) 971A ε_{Nd} (bold line and filled circles, Osborne et al. (2008)), $\delta^{18}O_{G.\ ruber}$ (faint line, Cane et al., 2002; Rohling et al., 2002). b) 967C ε_{Nd} (bold line and filled diamonds) and $\delta^{18}O_{G.\ ruber}$ (faint line), both from Scrivner et al. (2004). c) LC21 ε_{Nd} (bold line and open circles, this study) and $\delta^{18}O_{G.\ ruber}$ (faint line, Rohling et al., 2002). Vertical error bars on ε_{Nd} data are 2σ. Horizontal bars show range of depths of the samples for each data point. For LC21 and 967C, a further 1 cm x-axis uncertainty is added to account for errors associated with correlation to 971A (Marino et al., 2007).

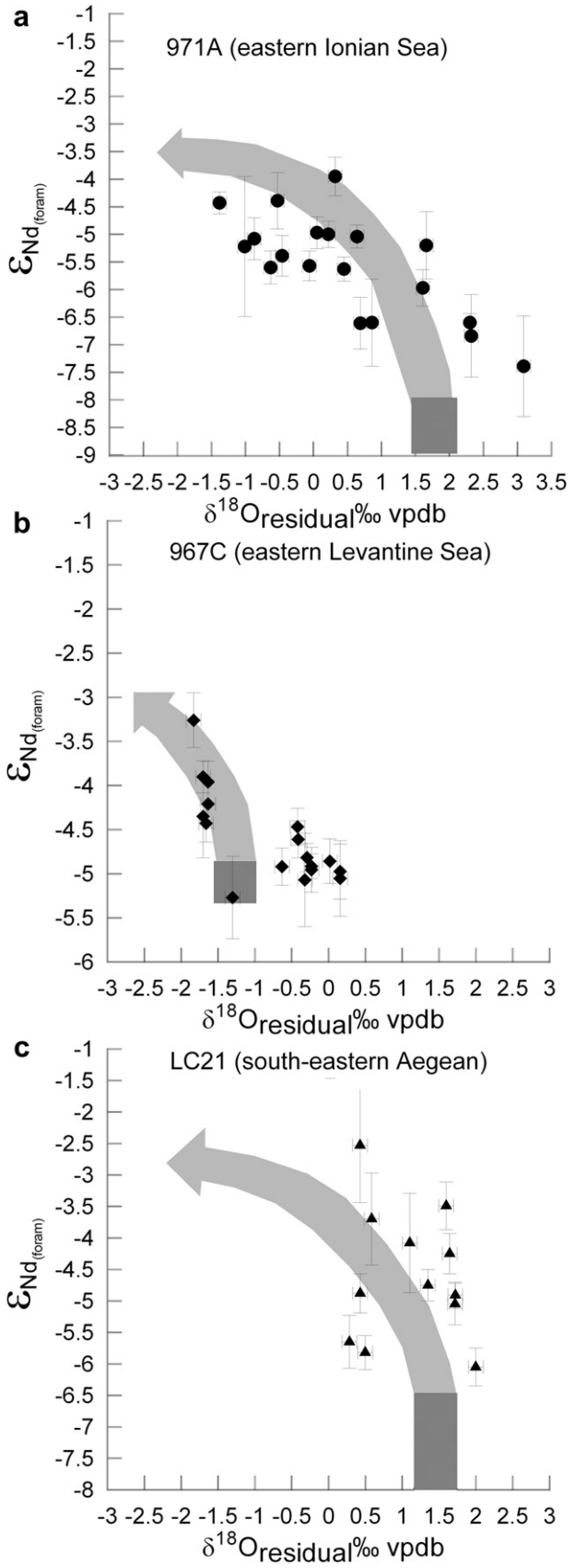

Fig. 5. ε_{Nd} versus $\delta^{18}O$ residuals for planktonic foraminifera in a) 971A, b) 967C and c) LC21. The data for 967C is from Scrivner et al. (2004). For a) and c), $\delta^{18}O_{residual}$ was calculated by normalising the published records (Cane et al., 2002; Rohling et al., 2002 ; Marino et al., 2007) to present-day temperature and $\delta^{18}O$ for 65–70 m water depth for the closest available data point in the World Ocean Database (Boyer et al., 2006) and the Global $\delta^{18}O$ Database (Gat et al., 1996; Pierre, 1999; Schmidt et al., 1999). At the level of S5, alkenone temperatures (Rohling et al., 2002; Marino et al., 2007) were used to remove the temperature effect from the measured $\delta^{18}O_{foram}$ signal, and sea-level change from Rohling et al. (2008) was used to remove ice-volume changes. Also shown on the figures are grey boxes indicating the estimated 'ambient', or 'non-sapropel' Mediterranean conditions (Gat et al., 1996; Pierre, 1999; Tachikawa et al., 2004) and broad grey arrows showing the generalized position of mixing curves between these end-members and an assumed North African freshwater input with Nd concentration of 200–300 pmol/kg and ε_{Nd} between −1 and −2 (Scrivner et al., 2004; Osborne et al., 2008) and $\delta^{18}O$ around −8 to −10 (Rohling et al., 2004).

contributes up to 22% of the Nile River summer discharge and 24.5% of the annual sediment (Adamson et al., 1980). Although it would appear that the White Nile is a contender for a non-radiogenic source of freshwater, it is difficult to imagine a situation where this tributary is affected by an increase in monsoon extent, without a corresponding increase in the contribution from the Blue Nile and Atbara, which are currently strongly affected by the African summer monsoon system. 971A does not have such a lag, suggesting that the ε_{Nd} and $\delta^{18}O$ signal in this core were from the same source. This instantaneous response of ε_{Nd} could indicate that dissolvable Nd was readily available when Libyan rivers were reactivated.

The lack of a sharp positive excursion in the LC21 ε_{Nd} record at the onset of the sapropel, and the subdued $\delta^{18}O_{G.\ ruber}$ anomaly when compared with 971A (Cane et al., 2002; Rohling et al., 2002; Marino et al., 2007) (Fig. 4), are consistent with a radiogenic freshwater source distal to the Aegean. LC21 is in the path of northward flowing surface waters from the Levantine Basin at present (Theocharis et al., 2002) and that was likely the case also during S5 (Marino et al., 2007). This places the site further "downstream" from inputs to the southern Mediterranean than both 971A and 967C.

Because ambient surface water ε_{Nd} in the southeast Aegean is not well constrained, and could be anywhere between −5 and −8 (see Section 6.2), it is difficult to assess the exact magnitude of the observed change in ε_{Nd} across S5 relative to the changes reported for 971A and 967C. If 'ambient' ε_{Nd} was −8, then surface waters in the southeastern Aegean had already shifted to a more radiogenic Nd composition before the onset of sapropel conditions, and remained radiogenic throughout S5 deposition. This would also suggest that ε_{Nd} and $\delta^{18}O_{G.\ ruber}$ were not directly linked, as they appear to be in the Ionian (971A), and to a lesser extent in the Levantine (967C), Seas. If 'ambient' ε_{Nd} was closer to −5, as for eastern Levantine surface water, then the early change in $\delta^{18}O_{G.\ ruber}$ was accompanied by little change in ε_{Nd}. A greater amount of direct precipitation over the Aegean is another possible source of freshwater, as this would not contribute any Nd (Kallel et al., 1997; Bar-Matthews et al., 2003). In all cases, there is no strong evidence for any shift towards less radiogenic Nd, as would be required by an increased input from European and Turkish rivers draining from the NBEM (Nd of −10 and −6 ε_{Nd} respectively, Frost et al., 1986). This supports conclusions already drawn on the basis of a comparison of the $\delta^{18}O_{G.\ ruber}$ and sea surface temperature data in 971A and LC21 (Marino et al., 2007). Before, and at the onset of, the sapropel event $\delta^{18}O_{G.\ ruber}$ at both sites show very similar patterns. However, despite the fact that alkenone-derived sea surface temperatures are similar in both locations, within S5 $\delta^{18}O_{G.\ ruber}$ is 1‰ heavier in the Aegean than in the Ionian (Marino et al., 2007). The most reasonable explanation for such isotopic offset is the advection of monsoon-fuelled freshwater from the North African margin to the southeastern Aegean following the basin counterclockwise surface circulation (Marino et al., 2007). Along this path surface waters would be exposed to the highly evaporative conditions of the southeastern Mediterranean (Rohling, 1999) and mixing, thereby

explaining the heavier $\delta^{18}O_{G.\ ruber}$ found in LC21 (Marino et al., 2007). Nd isotopes are, of course, unaffected by evaporation. The fact that ε_{Nd} is, if anything, more radiogenic during the entirety of the S5 oxygen isotope anomaly at LC21 than at the present-day, is generally consistent with the advection of radiogenic Nd from the African margin, accompanied by some dilution of the signal during mixing with other water masses.

The ε_{Nd} excursion towards the top of LC21 S5 sediments is the most radiogenic measurement of all three records. The total range of ε_{Nd} in LC21, at 2.8 ± 0.9 ε units, is larger than that seen for 967C (1.7 ε units) (Scrivner et al., 2004), but smaller than the 4–5 ε units change in 971A (Osborne et al., 2008). This excursion in LC21 is difficult to explain in terms of a radiogenic freshwater input which is closer to the southeastern Aegean than the eastern Levantine, and which is only apparent in the upper parts of the sapropel. Turkish and European rivers have ε_{Nd} of −6 and −10 respectively (Frost et al., 1986), so would not be able to cause a positive ε_{Nd} excursion. One possibility is that there was a change in Mediterranean surface circulation, bringing radiogenic waters from the Gulf of Sirte northwestwards into the Aegean rather than first travelling anticlockwise around the perimeter of the Ionian and Levantine Seas. Investigating the response of Mediterranean surface circulation to freshwater inputs is an important target for future study.

6.4. Mixing relationships: $\delta^{18}O$ versus ε_{Nd}

Fig. 5 presents a plot of ε_{Nd} versus the $\delta^{18}O_{residual}$ (i.e. with the temperature and ice-volume signals removed to leave only the freshwater signal – see caption to Fig. 5 for details) for foraminiferal measurements in the depth interval of S5 in cores 971A, 967C and LC21. In each case the best estimate of the ambient non-sapropel conditions is shown with a grey square (see caption to Fig. 5 for details). Mixing between this ambient condition and an end-member with ε_{Nd} around −1 to −2 (as typifies both the Nile outflow and a putative ancient Libyan River: Scrivner et al., 2004; Osborne et al., 2008) and a $\delta^{18}O$ around −8 to −10 (a value used by Rohling et al., 2004 for modeling the effects of monsoon flooding) is indicated by the broad grey arrow. The exact trajectories of these arrows imply a concentration of Nd in the riverine end-member of around 200 pmol/kg.

The model implicit in Fig. 5 is that the foraminiferal data can be explained solely by mixing between an "ambient" extra-sapropel Mediterranean end-member and a second end-member originating in an enhanced freshwater source to the Mediterranean, with a distinct ε_{Nd}. The approach is complicated by the difficulty in estimating the ambient conditions outside the sapropel, particularly for $\delta^{18}O$ for which two additional signals over and above that due to freshwater variations must be removed. Thus, the Mediterranean end-members defined by the data arrays are variably shifted from the estimated ambient Mediterranean conditions, a feature that could be of interpretive significance or could be due to the inherent uncertainty in estimating these ambient conditions. Nonetheless, several features of these diagrams are noteworthy.

Firstly, and as noted earlier, the LC21 data do not require a noticeable unradiogenic source of Nd to the Mediterranean, as might be derived from the NBEM, during S5. Recently, pollen-based reconstructions have suggested that precipitation and, in turn, river runoff increased considerably over the northern Aegean borderlands at the onset of the deposition of the weakly developed sapropel S1 (Kotthoff et al., 2008). Accordingly, these authors conclude that runoff over the northern Aegean borderlands might have played a role in the positive shift of the eastern Mediterranean freshwater balance that led to sapropel S1 deposition (Casford et al., 2002; De Lange et al., 2008). Our study, however, suggests that during a much more extreme sapropel event, the Last Interglacial sapropel S5, the freshwater inputs from the NBEM may have been negligible, at least when compared to the massive volumes of freshwater discharged along the wider North African margin (Rohling et al., 2002, 2004; Osborne et al., 2008). Summer aridity in the eastern Mediterranean, caused by adiabatic descent over the eastern Mediterranean (Rodwell and Hoskins, 1996) may have intensified during insolation minimia, leading to reduced precipitation in the NBEM (Tzedakis et al., 2009). Our results suggest that the return to mid-latitude westerly influence during winter did not bring sufficient precipitation to the NBEM to significantly alter the Nd composition of surface waters in the southeast Aegean.

Secondly, the three sites, on this diagram, show somewhat contrasting behaviour. In the Ionian Sea (971A) $\delta^{18}O$ and ε_{Nd} show rather coherent relationships for almost all the data. In contrast, and as noted by Scrivner et al. (2004), the initial stages of S5 in 967C (eastern Levantine Sea) exhibit a substantial shift in $\delta^{18}O$ with little change in ε_{Nd}. Finally, the LC21 record is again different from the other two in that it exhibits the least overall variability in $\delta^{18}O$ while showing substantial variation in ε_{Nd}. All three of these observations refer to the relationships among the actual data, and hold true regardless of the exact position of the ambient Mediterranean end-member relative to these data arrays. It seems likely that our two tracers, ε_{Nd} and $\delta^{18}O$, would display the most coherent behaviour proximal to any source of freshwater. Given the rather complex oceanographic processes that lead to non-conservativity in both tracers in surface waters of the open ocean (evaporation for $\delta^{18}O$, scavenging and other particulate interactions for ε_{Nd}, Rohling and Bigg, 1998; Tachikawa et al., 2004; Jeandel et al., 2007), it also seems likely that such coherence might disappear more distally. As such, the general breakdown in the coherence of the two signals the further round the eastern Mediterranean circulation one proceeds is perhaps what is to be expected. Though this observation is consistent with the idea of a single Saharan source of freshwater to the Mediterranean upstream from 971A during S5, confirmation depends on a modeling approach that can fully simulate the non-conservative processes that govern Nd and oxygen in the surface of the eastern Mediterranean.

7. Conclusions

The Ionian Sea foraminiferal record (971A) shows a distinct change towards more radiogenic ε_{Nd} at the base of sapropel S5, accompanying a significant move towards lighter $\delta^{18}O_{G.\ ruber}$. This is in contrast to the record from the eastern Levantine Sea (967C), which shows a much smaller change towards lighter $\delta^{18}O_{G.\ ruber}$ at the base of the sapropel, and little change in ε_{Nd}. The lack of a shift towards an unradiogenic Nd signal in the Aegean Sea core LC21 is inconsistent with the idea that there was a significant increase in freshwater supply to the eastern Mediterranean during S5 from the northern borderlands of the Eastern Mediterranean. There is a strong shift towards more radiogenic Nd at the top of the sapropel in the southeastern Aegean, which is difficult to explain in terms of any local source.

The relative change in ε_{Nd} during the sapropel is greater in the Ionian Sea record than the eastern Levantine Sea record, suggesting a source of radiogenic freshwater more proximal to the western core, for which monsoon runoff from the wider North African margin is a strong contender, based on the characterisation of Nd in these ancient water courses (Osborne et al., 2008). Coherency between the $\delta^{18}O_{G.\ ruber}$ and ε_{Nd} data, as revealed by model mixing diagrams, is at its greatest in the Ionian Sea core. This coherency decreases in the eastern Levantine Sea and especially into the Aegean. This geographic pattern is also conceptually consistent with the proximity to the Ionian Sea of a high ε_{Nd} freshwater source.

Though a quantitative test must await a model that can incorporate both the physical circulation of the eastern Mediterranean and the marine geochemical processes impacting Nd, the disappearance of the coherency between the two proxies may be due to processes operating during transport of both signals around the surface anticlockwise gyre.

Acknowledgements

This research was supported by a Natural Environment Research Council (United Kingdom) studentship (to A. H. O.). We thank two anonymous reviewers and Tina van de Flierdt (Guest Editor) for their constructive comments on an earlier version of the manuscript.

References

Adamson, D.A., Gasse, F., Street, F.A., Williams, M.A.J., 1980. Late Quaternary history of the Nile. Nature 288 (5786), 50–55.

Bar-Matthews, M., Ayalon, A., Kaufman, A., 2000. Timing and hydrological conditions of sapropel events in the Eastern Mediterranean, as evident from speleothems, Soreq cave, Israel. Chemical Geology 169 (1–2), 145–156.

Bar-Matthews, M., Ayalon, A., Gilmour, M., Matthews, A., Hawkesworth, C.J., 2003. Sea–land oxygen isotopic relationships from planktonic foraminifera and speleothems in the Eastern Mediterranean region and their implication for paleorainfall during interglacial intervals. Geochimica et Cosmochimica Acta 67 (17), 3181–3199.

Bau, M., Koschinsky, A., Dulski, P., Hein, J.R., 1996. Comparison of the partitioning behaviours of yttrium, rare earth elements, and titanium between hydrogenetic marine ferromanganese crusts and seawater. Geochimica et Cosmochimica Acta 60 (10), 1709–1725.

Boyer, T.P., Antonov, J.I., Garcia, H., Johnson, D.R., Locarnini, R.A., Mishonov, A.V., Pitcher, M.T., Baranova, O.K., Smolyar, I., 2006. World ocean database 2005. In: Levitus, S. (Ed.), NOAA Atlas NESDIS 60. U.S. Government Printing Office, Washington D.C.

Boyle, E.A., 1983. Manganese carbonate overgrowths on foraminifera tests. Geochimica et Cosmochimica Acta 47 (10), 1815–1819.

Boyle, E.A., Keigwin, L.D., 1985. Comparison of Atlantic and Pacific paleochemical records for the last 215,000 years – changes in deep ocean circulation and chemical inventories. Earth and Planetary Science Letters 76 (1–2), 135–150.

Burton, K.W., Vance, D., 2000. Glacial–interglacial variations in the neodymium isotope composition of seawater in the Bay of Bengal recorded by planktonic foraminifera. Earth and Planetary Science Letters 176 (3–4), 425–441.

Cane, T., Rohling, E.J., Kemp, A.E.S., Cooke, S., Pearce, R.B., 2002. High-resolution stratigraphic framework for Mediterranean sapropel S5: defining temporal relationships between records of Eemian climate variability. Palaeogeography, Palaeoclimatology, Palaeoecology 183 (1–2), 87–101.

Casford, J.S.L., Rohling, E.J., Abu-Reid, R., Cooke, S., Fontanier, C., Leng, M., Lykousis, V., 2002. Circulation changes and nutrient concentrations in the late Quaternary Aegean Sea: a nonsteady state concept for sapropel formation. Paleoceanography 17 (2).

CIESM, 2009. Dynamics of Mediterranean deep waters. In: Briand, F. (Ed.), CIESM Workshop Monographs, vol. 38, Monaco, 132 pp.

Claussen, M., Kubatzki, C., Brovkin, V., Ganopolski, A., Hoelzmann, P., Pachur, H.J., 1999. Simulation of an abrupt change in Saharan vegetation in the mid-Holocene. Geophysical Research Letters 26 (14), 2037–2040.

Cramp, A., O'Sullivan, G., 1999. Neogene sapropels in the Mediterranean: a review. Marine Geology 153 (1–4), 11–28.

Cramp, A., Collins, M., West, R., 1988. Late Pleistocene Holocene sedimentation in the Nw Aegean Sea – a paleoclimatic paleoceanographic reconstruction. Palaeogeography, Palaeoclimatology, Palaeoecology 68 (1), 61–77.

De Lange, G.J., Thomson, J., Reitz, A., Slomp, C.P., Principato, M.S., Erba, E., Corselli, C., 2008. Synchronous basin-wide formation and redox-controlled preservation of a Mediterranean sapropel. Nature Geoscience 1 (9), 606–610.

Erez, J., 2003. The source of ions for biomineralization in foraminifera and their implication for paleoceanographic proxies. Reviews in Mineralogy and Geochemistry 54, 115–149.

Evans, J.S., 2003. Principles of molecular biology and biomacromolecular chemistry. In: Dove, P.M., de Yoreo, J.J., de Yoreo, S. (Eds.), Biomineralization, vol. 54, pp. 31–56.

Falkowski, P.G., Barber, R.T., Smetacek, V., 1998. Biogeochemical controls and feedbacks on ocean primary production. Science 281 (5374), 200–206.

Fontugne, M., Arnold, M., Labeyrie, L., Paterne, M., Calvert, S.E., Duplessy, J.C., 1994. Palaeoenvironment sapropel chronology and Nile river discharge during the last 20 000 years as indicated by deep sea sediment records in the Eastern Mediterranean. In: Bar-Yosef, O., Kra, R.S. (Eds.), Late Quaternary Chronology and Paleoclimates of the Eastern Mediterranean. Radiocarbon, 75–88.

Foster, G.L., Vance, D., 2006. Negligible glacial–interglacial variation in continental chemical weathering rates. Nature 444 (7121), 918–921.

Frank, M., 2002. Radiogenic isotopes: tracers of past ocean circulation and erosional input. Reviews of Geophysics 40 (1).

Freydier, R., Michard, A., De Lange, G., Thomson, J., 2001. Nd isotopic compositions of Eastern Mediterranean sediments: tracers of the Nile influence during sapropel S1 formation? Marine Geology 177 (1–2), 45–62.

Frost, C.D., Onions, R.K., Goldstein, S.L., 1986. Mass Balance for Nd in the Mediterranean-Sea. Chemical Geology 55 (1–2), 45–50.

Gat, J.R., Shemesh, A., Tziperman, E., Hecht, A., Georgopoulos, D., Basturk, O., 1996. The stable isotope composition of waters of the eastern Mediterranean Sea. Journal of Geophysical Research-Oceans 101 (C3), 6441–6451.

Goldstein, S.B., Hemming, S.R., 2003. Long-lived isotopic tracers in oceanography, paleoceanography and ice-sheet dynamics. In: Holland, H.D., Turekian, K.K. (Eds.), Treatise on Geochemistry, vol. 6. Elsevier, Oxford, pp. 453–489.

Grousset, F.E., Rognon, P., Coudegaussen, G., Pedemay, P., 1992. Origins of Peri-Saharan dust deposits traced by their Nd and Sr isotopic composition. Palaeogeography, Palaeoclimatology, Palaeoecology 93 (3–4), 203–212.

Haley, B.A., Klinkhammer, G.P., 2002. Development of a flow-through system for cleaning and dissolving foraminiferal tests. Chemical Geology 185 (1–2), 51–69.

Haley, B.A., Klinkhammer, G.P., Mix, A.C., 2005. Revisiting the rare earth elements in foraminiferal tests. Earth and Planetary Science Letters 239 (1–2), 79–97.

Henry, F., Jeandel, C., Dupre, B., Minster, J.F., 1994. Particulate and dissolved Nd in the Western Mediterranean-Sea – sources, fate and budget. Marine Chemistry 45 (4), 283–305.

Hilgen, F.J., Krijgsman, W., Langereis, C.G., Lourens, L.J., 1997. Breakthrough made in dating the geological record. Eos Transactions American Geophysical Union 78 (28), 287–289.

Jeandel, C., Arsouze, T., Lacan, F., Techine, P., Dutay, J.C., 2007. Isotopic Nd compositions and concentrations of the lithogenic inputs into the ocean: a compilation, with an emphasis on the margins. Chemical Geology 239 (1–2), 156–164.

Jolly, D., Harrison, S.P., Damnati, B., Bonnefille, R., 1998. Simulated climate and biomes of Africa during the late Quaternary: comparison with pollen and lake status data. Quaternary Science Reviews 17 (6–7), 629–657.

Kallel, N., Paterne, M., Duplessy, J.C., VergnaudGrazzini, C., Pujol, C., Labeyrie, L., Arnold, M., Fontugne, M., Pierre, C., 1997. Enhanced rainfall in the Mediterranean region during the last sapropel event. Oceanologica Acta 20 (5), 697–712.

Kotthoff, U., Pross, J., Muller, U.C., Peyron, O., Schmiedl, G., Schulz, H., Bordon, A., 2008. Climate dynamics in the borderlands of the Aegean Sea during formation of sapropel S1 deduced from a marine pollen record. Quaternary Science Reviews 27 (7–8), 832–845.

Krom, M.D., Cliff, R.A., Eijsink, L.M., Herut, B., Chester, R., 1999a. The characterisation of Saharan dusts and Nile particulate matter in surface sediments from the Levantine basin using Sr isotopes. Marine Geology 155 (3–4), 319–330.

Krom, M.D., Michard, A., Cliff, R.A., Strohle, K., 1999b. Sources of sediment to the Ionian Sea and western Levantine basin of the Eastern Mediterranean during S-1 sapropel times. Marine Geology 160 (1–2), 45–61.

Kutzbach, J.E., Guetter, P.J., 1986. The Influence of changing orbital parameters and surface boundary – conditions on climate simulations for the past 18000 years. Journal of the Atmospheric Sciences 43 (16), 1726–1759.

Kutzbach, J.E., Liu, Z., 1997. Response of the African monsoon to orbital forcing and ocean feedbacks in the middle Holocene. Science 278 (5337), 440–443.

Larrasoaña, J.C., Roberts, A.P., Rohling, E.J., Winklhofer, M., Wehausen, R., 2003. Three million years of monsoon variability over the northern Sahara. Climate Dynamics 21 (7–8), 689–698.

Lionello, P., Malanotte-Rizzoli, P., Boscolo, R., Alpert, P., Artale, V., Li, L., Luterbacher, J., May, W., Trigo, R., Tsimplis, M., Ulbrich, U., Xoplaki, E., 2006. The Mediterranean climate: an overview of the main characteristics and issues. In: Lionello, P., Malanotte-Rizzoli, P., Boscolo, R. (Eds.), Mediterranean Climate Variability. Elsevier, Amsterdam, The Netherlands, pp. 1–26.

Lipps, J.H., 1973. Test structure in foraminifera. Annual Review of Microbiology 27, 471–488.

Malanotte-Rizzoli, P., Manca, B.B., d'Alcala, M.R., Theocharis, A., Brenner, S., Budillon, G., Ozsoy, E., 1999. The Eastern Mediterranean in the 80s and in the 90s: the big transition in the intermediate and deep circulations. Dynamics of Atmospheres and Oceans 29 (2–4), 365–395.

Marino, G., Rohling, E.J., Rijpstra, W.I.C., Sangiorgi, F., 2007. Aegean Sea as driver of hydrographic and ecological changes in the eastern Mediterranean. Geology 35 (8), 675–678.

Martínez-Botí, M.A., Vance, D., Mortyn, P.G., 2009. Nd/Ca ratios in plankton-towed and core top foraminifera: confirmation of the water column acquisition of Nd. Geochemistry, Geophysics, Geosystems 10.

Martrat, B., Grimalt, J.O., Lopez-Martinez, C., Cacho, I., Sierro, F.J., Flores, J.A., Zahn, R., Canals, M., Curtis, J.H., Hodell, D.A., 2004. Abrupt temperature changes in the Western Mediterranean over the past 250,000 years. Science 306 (5702), 1762–1765.

McCauley, J.F., Schaber, G.G., Breed, C.S., Grolier, M.J., Haynes, C.V., Issawi, B., Elachi, C., Blom, R., 1982. Subsurface valleys and geoarcheology of the eastern Sahara revealed by shuttle radar. Science 218 (4576), 1004–1020.

McCauley, J.F., Breed, C.S., Issawi, B., Schaber, G.G., 1995. Space Radar Lab (SRL-1). Studies of the paleodrainages of the astern Sahara. Special Issue IEEE Transactions Geoscience Remote Sensing 33, 624–647.

Olausson, E., 1961. Studies of deep-sea cores. In: Reports of the Swedish Deep Sea Expedition, 1947–1948, vol. 8, pp. 335–391.

Osborne, A.H., Vance, D., Rohling, E.J., Barton, N., Rogerson, M., Fello, N., 2008. A humid corridor across the Sahara for the migration of early modern humans out

of Africa 120,000 years ago. Proceedings of the National Academy of Sciences of the United States of America 105 (43), 16444–16447.
Pachur, H.J., Altmann, N., 2006. Die Ostsahara im Spätquartär. Springer, Berlin-Heidelberg.
Palmer, M.R., 1985. Rare-Earth elements in foraminifera tests. Earth and Planetary Science Letters 73 (2–4), 285–298.
Pierre, C., 1999. The oxygen and carbon isotope distribution in the Mediterranean water masses. Marine Geology 153 (1–4), 41–55.
Pinardi, N., Masetti, E., 2000. Variability of the large scale general circulation of the Mediterranean Sea from observations and modelling: a review. Palaeogeography, Palaeoclimatology, Palaeoecology 158 (3–4), 153–174.
Piotrowski, A.M., Goldstein, S.L., Hemming, S.R., Fairbanks, R.G., 2005. Temporal relationships of carbon cycling and ocean circulation at glacial boundaries. Science 307 (5717), 1933–1938.
Pujol, C., Vergnaud-Grazzini, C., 1995. Distribution patterns of live planktic foraminifers as related to regional hydrography and productive systems of the Mediterranean-Sea. Marine Micropaleontology 25 (2–3), 187–217.
Ren, H., Sigman, D.M., Meckler, A.N., Plessen, B., Robinson, R.S., Rosenthal, Y., Haug, G.H., 2009. Foraminiferal isotope evidence of reduced nitrogen fixation in the ice age Atlantic Ocean. Science 323 (5911), 244–248.
Reynolds, B.C., Sherlock, S.C., Kelley, S.P., Burton, K.W., 2004. Radiogenic isotope records of Quaternary glaciations: changes in the erosional source and weathering processes. Geology 32 (10), 861–864.
Riebe, C.S., Kirchner, J.W., Finkel, R.C., 2004. Erosional and climatic effects on long-term chemical weathering rates in granitic landscapes spanning diverse climate regimes. Earth and Planetary Science Letters 224 (3–4), 547–562.
Rodwell, M.J., Hoskins, B.J., 1996. Monsoons and the dynamics of deserts. Quarterly Journal of the Royal Meteorological Society 122 (534), 1385–1404.
Roether, W., Manca, B.B., Klein, B., Bregant, D., Georgopoulos, D., Beitzel, V., Kovacevic, V., Luchetta, A., 1996. Recent changes in eastern Mediterranean deep waters. Science 271 (5247), 333–335.
Roether, W., Klein, B., Manca, B.B., Theocharis, A., Kioroglou, S., 2007. Transient Eastern Mediterranean deep waters in response to the massive dense-water output of the Aegean Sea in the 1990s. Progress in Oceanography 74, 540–571.
Rohling, E.J., 1994. Review and new aspects concerning the formation of Eastern Mediterranean sapropels. Marine Geology 122 (1–2), 1–28.
Rohling, E.J., 1999. Environmental controls on salinity and $d^{18}O$ in the Mediterranean. Paleoceanography 14, 706–715.
Rohling, E.J., Hilgen, F.J., 1991. The Eastern Mediterranean climate at times of sapropel formation – a review. Geologie En Mijnbouw 70 (3), 253–264.
Rohling, E.J., Bigg, G.R., 1998. Paleosalinity and delta O-18: a critical assessment. Journal of Geophysical Research-Oceans 103 (C1), 1307–1318.
Rohling, E.J., De Rijk, S., 1999. Holocene climate optimum and last glacial maximum in the Mediterranean: the marine oxygen isotope record (vol 153, pg 57, 1999). Marine Geology 161 (2–4), 385–387.
Rohling, E.J., Cane, T.R., Cooke, S., Sprovieri, M., Bouloubassi, I., Emeis, K.C., Schiebel, R., Kroon, D., Jorissen, F.J., Lorre, A., Kemp, A.E.S., 2002. African monsoon variability during the previous interglacial maximum. Earth and Planetary Science Letters 202 (1), 61–75.
Rohling, E.J., Sprovieri, M., Cane, T., Casford, J.S.L., Cooke, S., Bouloubassi, I., Emeis, K. C., Schiebel, R., Rogerson, M., Hayes, A., Jorissen, F.J., Kroon, D., 2004. Reconstructing past planktic foraminiferal habitats using stable isotope data: a case history for Mediterranean sapropel S5. Marine Micropaleontology 50 (1–2), 89–123.
Rohling, E.J., Hopmans, E.C., Damste, J.S.S., 2006. Water column dynamics during the Last Interglacial anoxic event in the Mediterranean (sapropel S5). Paleoceanography 21 (2).
Rohling, E.J., Grant, K., Hemleben, C., Siddall, M., Hoogakker, B.A.A., Bolshaw, M., Kucera, M., 2008. High rates of sea-level rise during the Last Interglacial period. Nature Geoscience 1 (1), 38–42.
Rossignol-Strick, M., 1983. African Monsoons, an immediate climate response to orbital insolation. Nature 304 (5921), 46–49.
Rossignol-Strick, M., 1985. Mediterranean Quaternary sapropels, an immediate response of the African monsoon to variation of insolation. Palaeogeography, Palaeoclimatology, Palaeoecology 49, 237–263.
Rossignol-Strick, M., Nesteroff, W., Olive, P., Vergnaudgrazzini, C., 1982. After the deluge – Mediterranean stagnation and sapropel formation. Nature 295 (5845), 105–110.
Roussenov, V., Stanev, E., Artale, V., Pinardi, N., 1995. A seasonal model of the Mediterranean-Sea general-circulation. Journal of Geophysical Research-Oceans 100 (C7), 13515–13538.
Ryan, W., 1972. Stratigraphy of Late Quaternary sediments in the Eastern Mediterranean. In: Stanley, D.J. (Ed.), The Mediterranean Sea. Dowden, Hutchinson and Ross, Stroudsbury, PA, pp. 1–765.
Schmidt, G.A., Bigg, G.R., Rohling, E.J., 1999. Global Seawater Oxygen-18 Database. http://data.giss.nasa.gov/o18data/.
Scrivner, A.E., 2005. Palaeoclimate and circulation in the Mediterranean: the importance of the River Nile. Ph.D. Thesis. Royal Holloway, University of London.
Scrivner, A.E., Vance, D., Rohling, E.J., 2004. New neodymium isotope data quantify Nile involvement in Mediterranean anoxic episodes. Geology 32 (7), 565–568.
Skliris, N., Sofianos, S., Lascaratos, A., 2007. Hydrological changes in the Mediterranean Sea in relation to changes in the freshwater budget: a numerical modelling study. Journal of Marine Systems 65 (1–4), 400–416.
Sonntag, C., Klitzsch, E., Lohnert, E.P., El-Shazly, E.M., Munnich, K.O., Junghans, C., Thorweihe, U., Weistroffer, K., Swailem, F.M., 1978. Paleoclimatic information from deuterium and oxygen-18 in carbon-14-dated north Saharan groundwaters. Isotope Hydrology. International Atomic Energy Agency, Vienna. 569–580.
Sperling, M., Schmiedl, G., Hemleben, C., Emeis, K.C., Erlenkeuser, H., Grootes, P.M., 2003. Black Sea impact on the formation of eastern Mediterranean sapropel S1? Evidence from the Marmara Sea. Palaeogeography, Palaeoclimatology, Palaeoecology 190, 9–21.
Spivack, A.J., Wasserburg, G.J., 1988. Neodymium isotopic composition of the Mediterranean outflow and the eastern North-Atlantic. Geochimica et Cosmochimica Acta 52 (12), 2767–2773.
Sprovieri, R., Di Stefano, E., Incarbona, A., Gargano, M.E., 2003. A high-resolution record of the last deglaciation in the Sicily Channel based on foraminifera and calcareous nannofossil quantitative distribution. Palaeogeography, Palaeoclimatology, Palaeoecology 202 (1–2), 119–142.
Sprovieri, R., Di Stefano, E., Incarbona, A., Oppo, D.W., 2006. Suborbital climate variability during Marine Isotopic Stage 5 in the central Mediterranean basin: evidence from calcareous plankton record. Quaternary Science Reviews 25 (17–18), 2332–2342.
Sultan, M., Sturchio, N., Hassan, F.A., Hamdan, M.A.R., Mahmood, A.M., ElAlfy, Z., Stein, T., 1997. Precipitation source inferred from stable isotopic composition of Pleistocene groundwater and carbonate deposits in the Western Desert of Egypt. Quaternary Research 48 (1), 29–37.
Tachikawa, K., Roy-Barman, M., Michard, A., Thouron, D., Yeghicheyan, D., Jeandel, C., 2004. Neodymium isotopes in the Mediterranean Sea: comparison between seawater and sediment signals. Geochimica et Cosmochimica Acta 68 (14), 3095–3106.
Theocharis, A., Nittis, K., Kontoyiannis, K., Papageorgiou, E., Balopoulos, E., 1999. Climatic changes in the Aegean Sea influence the Eastern Mediterranean thermohaline circulation (1986–1997). Geophysical Research Letters 26 (11), 1617–1620.
Theocharis, A., Klein, B., Nittis, K., Roether, W., 2002. Evolution and status of the Eastern Mediterranean Transient (1997–1999). Journal of Marine Systems 33, 91–116.
Tzedakis, P.C., 2007. Seven ambiguities in the Mediterranean palaeoenvironmental narrative. Quaternary Science Reviews 26 (17–18), 2042–2066.
Tzedakis, P.C., Palike, H., Roucoux, K.H., de Abreu, L., 2009. Atmospheric methane, southern European vegetation and low-mid latitude links on orbital and millennial timescales. Earth and Planetary Science Letters 277 (3–4), 307–317.
Vance, D., Burton, K., 1999. Neodymium isotopes in planktonic foraminifera: a record of the response of continental weathering and ocean circulation rates to climate change. Earth and Planetary Science Letters 173 (4), 365–379.
Vance, D., Thirlwall, M., 2002. An assessment of mass discrimination in MC-ICPMS using Nd isotopes. Chemical Geology 185 (3–4), 227–240.
Vance, D., Scrivner, A.E., Beney, P., Staubwasser, M., Henderson, G.M., Slowey, N.C., 2004. The use of foraminifera as a record of the past neodymium isotope composition of seawater. Paleoceanography 19 (2).
Vance, D., Teagle, D.A.H., Foster, G.L., 2009. Variable Quaternary chemical weathering fluxes and imbalances in marine geochemical budgets. Nature 458 (7237), 493–496.
Weldeab, S., Emeis, K.C., Hemleben, C., Siebel, W., 2002a. Provenance of lithogenic surface sediments and pathways of riverine suspended matter in the Eastern Mediterranean Sea: evidence from Nd-143/Nd-144 and Sr-87/Sr-86 ratios. Chemical Geology 186 (1–2), 139–149.
Weldeab, S., Emeis, K.C., Hemleben, C., Vennemann, T.W., Schulz, H., 2002b. Sr and Nd isotope composition of Late Pleistocene sapropels and nonsapropelic sediments from the Eastern Mediterranean Sea: implications for detrital influx and climatic conditions in the source areas. Geochimica et Cosmochimica Acta 66 (20), 3585–3598.
Yu, G., Harrison, S.P., 1996. An evaluation of the simulated water balance of Eurasia and northern Africa at 6000 y BP using lake status data. Climate Dynamics 12 (11), 723–735.
Zanchetta, G., Drysdale, R.N., Hellstrom, J.C., Fallick, A.E., Isola, I., Gagan, M.K., Pareschi, M.T., 2007. Enhanced rainfall in the Western Mediterranean during deposition of sapropel S1: stalagmite evidence from Corchia cave (Central Italy). Quaternary Science Reviews 26 (3–4), 279–286.